A Combined Numerical/Experimental Continuation Approach Applied to Nonlinear Rotor Dynamics

D. Rezgui, M. Lowenberg, and P. Bunniss

Department of Aerospace Engineering, University of Bristol, UK, BS8 1TR,
Djamel.Rezgui@bristol.ac.uk, m.lowenburg@bristol.ac.uk,
peter.bunniss@bristol.ac.uk

Summary. Presented with complex systems exhibiting nonlinear behaviour, engineers in industry may face difficulties in understanding the system, both from a mathematical modeling perspective and also when trying to set up representative experiments. Here, a systematic approach combining numerical and experimental parameter continuation is applied to the investigation of complex nonlinear rotor behaviour. The aim is to show the benefits of co-ordinating numerical and physical tests in order to build a mathematical model that adequately captures the system dynamics. In this study the problem involves a dynamical system operating in a nonlinear periodic manner, with constraints on its states and parameters. The system is an autogyro rotor for which the approach generates a simple mathematical model yielding multiple possible autorotative conditions not previously identified in a systematic way; it also provides an explanation for unsafe operating scenarios.

1 Introduction

The aeromechanical stability of a rotor is a complex nonlinear problem, which involves interactions between different sources of nonlinearity. We consider the rotor of an autogyro which, unlike in a helicopter, is not driven by a power source but is kept rotating by the air flow through it; an engine with propeller provides forward thrust. It is known that when operating in autorotation at high forward speeds, the rotor can undergo unstable flapping behaviour (which has resulted in accidents) but the mechanisms at play are not well understood.

A number of methods have previously been applied to the stability of helicopter blades, ranging from pure time history simulation (time integration techniques) to parametric resonance analysis, Floquet stability theory and perturbation methods. However, these depend on assumptions that may be questionable for autorotating rotors (where rotation rate is variable, whereas for a helicopter it can be considered fixed) and inadequate to cover their entire stability picture.

A.D. Fitt et al. (eds.), *Progress in Industrial Mathematics at ECMI 2008*,
Mathematics in Industry 15, DOI 10.1007/978-3-642-12110-4_21,

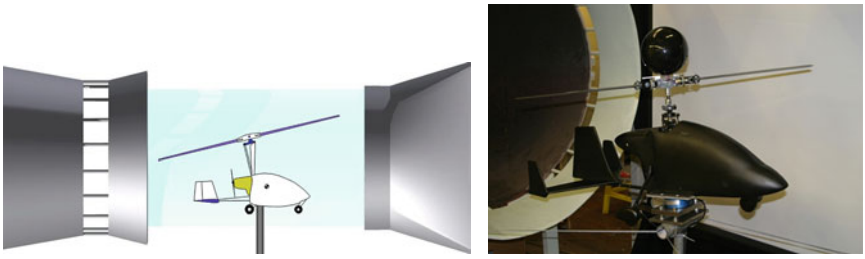

Fig. 1. Schematic view and photograph of autogyro rig in wind tunnel

Continuation and bifurcation methods have been successfully deployed to study the stability and control of a helicopter model, represented as a periodically forced nonlinear system with constant rotor speed [1]. The approach has now been extended to autorotating rotors using a relatively low order nonlinear mathematical model. These investigations using continuation and bifurcation methods [2,3] have confirmed that an autorotating rotor can undergo unstable behaviour. This includes the scenario observed in practice when the rotor is lightly loaded (i.e. at high speed).

To complement the numerical studies, an instrumented physical model of an autogyro was constructed for testing in a wind tunnel. The experiments were performed in the University of Bristol low-speed closed-return open-jet wind tunnel, with a 1.1 m jet diameter and maximum attainable velocity is about 33 m/s. Figure 1 depicts the rig in the tunnel.

The experimental rig [4] comprises a two-bladed teeter rotor of 1 m diameter, free to flap about a hinge located at the rotor shaft axis. An airframe similar to a production autogyro with an enclosed cockpit was constructed in order to cover the rotor support frame with an aerodynamically faired shape. The following measurements were taken from the rig: rotor blade flapping angle, pitch of each blade, rotor speed and azimuthal position and forces and moments acting on the rig. The signals measured on the rotating parts were transmitted to a computer outside the tunnel by wireless telemetry.

The rotor is modeled mathematically as a dynamical system in the form of a set of nonlinear ordinary differential equations. The rotor has two rigid blades and a 2-D individual blade element approach is used to model the aerodynamic loads on each. The blades are assumed to be rigidly connected and hence have one flapping degree of freedom. The lead-lag motion is captured in the rotational degree of freedom around the shaft axis; the flapping coordinate for the blades, β, is dependent on azimuth angle, ψ. The equations of motion for the rotor in both the flapping and the rotation senses are second order, giving a total of four rotor states (ψ, $\dot{\psi}$, β and $\dot{\beta}$); see for example [5].

The blades have no geometric twist or taper and the aerofoil profile is considered to be a NACA0015 section. Aerodynamic loads for each individual blade element are calculated numerically utilising nonlinear look-up tables for lift and drag coefficients of this aerofoil, defined from experimental data

for a 360° range of angle of attack [6]. The rotor inflow is captured via a 3-state Pitt–Peters dynamic wake model [7, 8], modified to account for the rotor being in autorotation. The total number of states (rotor and inflow dynamics) is seven. The parameters of interest here are the forward speed, V, and the longitudinal shaft angle, θ_{shaft}. Further details can be found in [4].

2 Experimental and Numerical Bifurcation Studies

The steady state periodic solutions and their stability are determined numerically from the 7-state mathematical model as parameters are varied, using the continuation and bifurcation software `Auto` [9]. Bifurcation diagrams generated from this model [3] have shown that unloaded rotors in autorotation are prone to instability. This is due to the branches of stable and unstable periodic orbits moving into closer proximity as the rotor shaft angle is reduced – which would be the case at higher speeds.

The first experimental runs in the present study entailed taking measurements at stable autorotative conditions over a range of wind speeds for different shaft angles, with other parameters fixed. Since the data is periodic with rotor azimuth position, average peak values for each cycle were computed over several runs. These peak values for both the rotational velocity and the flapping angle are plotted as filled circles in Fig. 2 for $\theta_{shaft} = 7°$; the solid curve fitted through these points is a stable limit cycle branch in this experimental bifurcation diagram. The multiple circles at each wind speed, especially for flapping angle, reveal the scatter in the readings from different runs.

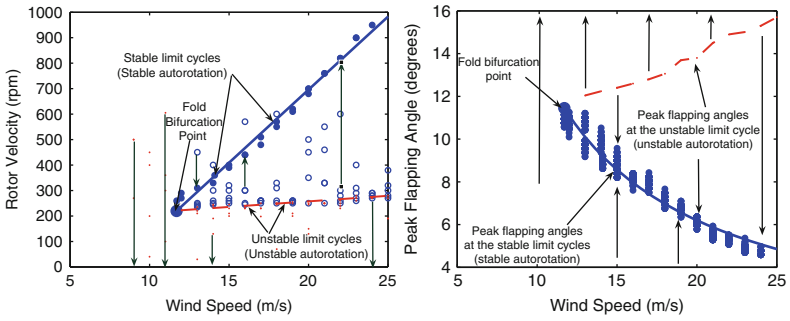

Fig. 2. Experimental bifurcation diagram of the rotational velocity (*left*) and the flapping angle (*right*) for $\theta_{shaft} = 7°$. *Solid circles* denote stable steady autorotation; the *solid curve* fitted to these points is the stable branch. *Hollow circles* represent initial points from which a stable steady autorotation state was achieved; *dots* show attempts where autorotation was not possible. The *dashed curve* represents the unstable autorotation steady state

Figure 2 illustrates that the rotational velocity increases almost linearly with the forward wind speed, while the flapping angle has an inverse relationship with the wind speed. The same trends are found for the other shaft angles tested. This shows that more flow goes through the rotor the faster it rotates, increasing the centrifugal stiffening and hence lowering the flapping angle. It is also clear that autorotation is not possible below a certain wind speed value (indicated as a fold bifurcation); to the left of this point, the rotor speed decays and the rotor flapping oscillation diverges until a safety mechanism is activated.

Next, the experiment was run to test the ability of the rotor to autorotate at wind speeds higher than the fold point but starting from low initial rotor velocities. For every shaft angle setting, rotor speed thresholds were found above which the rotor can achieve steady autorotation. The hollow circles in Fig. 2 illustrate attempts where a steady autorotation state was achieved from the initial condition (i.e. the trajectory evolved towards the solid circles). The dots are attempts leading to unstable rotation, characterised by diverging flapping and decaying rotational speed. By running a number of tests, it was possible to define a rotor speed boundary that separates the two scenarios: the dashed curve in Fig. 2. At this boundary, the behaviour of the rotor appears to be steady but due to flow disturbances it will diverge – either to the stable autorotation state or an unstable condition. This is interpreted as an unstable autorotation branch in this experimental bifurcation diagram.

To develop a deeper understanding of the nonlinear mechanisms underlying the rotor behaviour, we return to numerical continuation and bifurcation analysis of the mathematical model; this allows parameter dependence to be investigated beyond the limitations of the experiment (e.g. higher wind speed or flapping angles). Initially this did not yield a bifurcation diagram of the same shape as the experimental one, although stable and unstable branches were located. The experimental bifurcation diagram was therefore used to modify, or 'tune', the mathematical model with the aim of producing at least qualitatively the same behaviour. The numerical model uses a simple aerodynamic representation, neglecting characteristics such as blade tip and root losses, blade-to-blade interaction, unsteady aerodynamics, airframe and tunnel interaction effects, rotor downwash, etc. Also, friction acting on the rotor shaft is ignored. For simplicity, the model was adapted by incorporating a friction term in the rotation sense of the rotor to attempt to capture the effects of all unmodelled phenomena. The frictional term is formulated as a resisting torque assumed proportional to the rotational velocity; see [4]. The tuning of the coefficients in this term was performed to match rotor speed to experimental values.

Figure 3 depicts the bifurcation diagram obtained from the modified numerical model at various shaft angles. The shape of the stable autorotation branches are very similar to those obtained from experiment, although the fold bifurcation points are located at slightly higher wind speed values. These results illustrate how the essence of the stability of a rotor in autorotation can

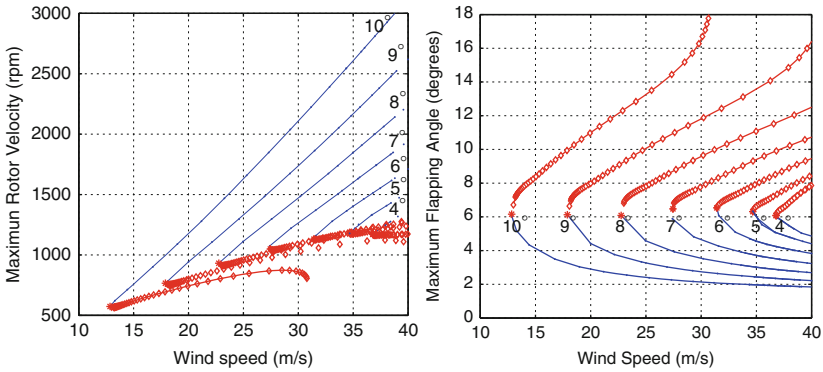

Fig. 3. Bifurcation diagram for the numerical rotor model at shaft angles of 4° to 10°. *Solid dotted curve* is stable; curve with *hollow diamonds* is unstable

be predicted to a high level, when continuation and bifurcation techniques are adapted, even though the numerical model is relatively simple. Furthermore, the figure shows that the wind speed value at which the fold bifurcation points exist increases as the shaft angle is reduced. Therefore, the boundary of rotor stability can be constructed by 2-parameter continuation (not shown), yielding the safe operating limits of the autogyro.

If the rotor flapping angles on both the stable and unstable branches are compared to those obtained from experiment, it is seen that their overall curve shapes are very similar. However, the amplitudes of the flapping angles computed are smaller than those of the physical rotor, particularly close to the bifurcation point. This is not unexpected since the model tuning was performed only for the rotor velocity state. The quantitative aspect of the analysis can be improved by incorporating a higher fidelity rotor model.

3 Conclusions

An example of a combined numerical-experimental approach to generating bifurcation diagrams has been shown to yield powerful information on the dynamics of a complex physical nonlinear system. The numerical results provide a qualitative framework to explain the experimental outcomes, which can in turn be used to validate the predictions and tune the model. In this case, an autorotating rotor was studied: a simple mathematical model was defined and then tuned using results from an experimental bifurcation diagram. Numerical continuation of this model showed, for the first time, the presence of both stable and unstable autorotation branches and their parameter dependence.

Results for other shaft angles (not shown) reveal that the smaller this angle is, the higher the wind speed below which autorotation cannot be sustained, i.e. the fold bifurcation occurs at higher forward speed. Thus a locus of fold

bifurcation points denotes the minimum permissible shaft angle required for autorotation at the corresponding wind speed: if the pilot reduces the shaft angle to decrease the lift coefficient for high speed flight, the rotor may enter an unstable condition where stable autorotation gives way to divergent flapping behaviour. In this way the bifurcation diagrams provide an explanation for high-speed autorotative instability as experienced in actual flight.

Future work will investigate following of unstable solutions directly in the experiment, as has already been achieved in a simpler nonlinear system [10].

Acknowledgments

This research was funded by *the Algerian Ministry for Higher Education and Scientific Research.*

References

1. Bedford, R., Lowenberg, M.: Flight dynamics analysis of periodically forced rotorcraft model. In: AIAA AFM Conference, number AIAA-2006-6634 (2006)
2. Rezgui, D., Bunniss, P.C., Lowenberg, M.H.: The stability of rotor blade flapping motion in autorotation using bifurcation and continuation analysis. Proceedings of 32nd European Rotorcraft Forum, 2006
3. Rezgui, D., Lowenberg, M.H., Bunniss, P.C.: Experimental and numerical analysis of the stability of an autogyro teetering rotor. Proceedings of the American Helicopter Society 64th Annual Forum, April 2008
4. Rezgui, D., Lowenberg, M., Bunniss, P.: Integrated experimental and numerical techniques in studying nonlinear rotor blade dynamics. In: ICNPAA Conference, 2008
5. Bramwell, A.R.S., Done, G., Balmford, D.: Bramwell's Helicopter Dynamics. Butterworth-Heinemann, Oxford (2001)
6. Sheldahl, R.E., Klimas, P.C.: Aerodynamic characteristics of seven airfoil sections through 180 degrees angle of attack for use in aerodynamic analysis of vertical axis wind turbines. SAND80-2114, Sandia National Laboratories, Albuquerque, New Mexico, March 1981
7. Chen, R.: A survey of nonuniform inflow models for rotorcraft flight dynamics and control applications. Vertica **14**(2), 147–184 (1990)
8. Peters, D., Morillo, J., Nelson, A.: New developments in dynamic wake modelling for dynamics applications. Proceedings of the American Helicopter Society 57th Annual Forum, May 2001
9. Doedel, E., Champneys, A., Fairgrieve, T., Kuznetsov, Y., Sandstede, B., Wang, X.: Auto97: Continuation and bifurcation software for ordinary differential equations. A.R.C. Technical Report C.P. No. 101 (14,757), http://indy.cs.concordia.ca/auto/, September 2007
10. Sieber, J., Gonzalez-Buelga, A., Neild, S., Wagg, D., Krauskopf, B.: Experimental continuation of periodic orbits through a fold. Phys. Rev. Lett. **100**(24), 244101 (2008)